IN-46-CR
191706
21P.

# THE BEHAVIOR OF THE ELECTRON DENSITY AND TEMPERATURE AT MILLSTONE HILL DURING THE EQUINOX TRANSITION STUDY SEPTEMBER 1984.

P.G. Richards[1], D.G. Torr[2], M.J. Buonsanto[3], K.L. Miller[4]

Short title: Electron Density and Temperature Behavior

[1] Computer Science Department and Center for Space Plasma and Aeronomic Research, University of Alabama in Huntsville, Huntsville Alabama

[2] Physics Department and Center for Space Plasma and Aeronomic Research, University of Alabama in Huntsville. Huntsville, Alabama

[3] Haystack Observatory, Massachusetts Institute of Technology, Westford, Massachusetts

[4] Physics Department and Center for Atmospheric and Space Sciences, Utah State University, Logan, Utah

**ABSTRACT:** In this paper, we simulate the ionospheric electron density and temperature variation during the equinox transition study in September 1984 and compare the results with measurements made at Millstone Hill. The agreement between the modeled and measured electron density and temperature for the quiet day (18 September) is very good but there are large differences on the day of the storm (19 September). On the storm day, the measured electron density decreases by a factor of 1.7 over the previous day, while the model density actually increases slightly. We attribute the model failure to an inadequate increase in the ratio of atomic oxygen to molecular neutral densities in the MSIS neutral atmosphere model, for this particular storm. A factor of 3-5 increase in the molecular to atomic oxygen density ratio at 300 km is needed to explain the observed decrease in electron density. We have also studied the effect of vibrationally excited $N_2$ on the electron density and found it to be small.

## INTRODUCTION

The complex behavior of the ionosphere during magnetic storms has been well reviewed by Prolss (1980). Because storm energy is initially deposited at high latitudes, the effects decrease with decreasing latitude. At high latitudes, the electron density is usually depressed while at low latitudes the density is more likely to be enhanced. The behavior is more complicated at midlatitudes, where the peak electron density may be enhanced (positive storm) or depressed (negative storm) depending on factors such as the local time of the storm onset. For example, in the storm of 21-22, 1973, The peak electron density at Brisbane, Australia exhibited a large daytime decrease in $N_mF_2$ while Pt. Arguello in North America at a similar latitude exhibited a large daytime increase in $N_mF_2$.

The storm onset at Brisbane was near sunrise while at Pt. Arguello it was near noon local time.

Seaton (1956) suggested that the negative phase of magnetic storms is associated with changes in the neutral composition and this explanation is supported by observations. Although diffusion plays an important role in the F region ionosphere, the peak electron density is approximately proportional to its chemical equilibrium value which is proportional to the ratio of atomic oxygen density to the molecular densities. The major source of $O^+$ is photoionization of atomic oxygen and the major sinks are recombination with the molecular species $O_2$ and $N_2$. Although the $N_2$ density is an order of magnitude larger than the $O_2$ density, the magnitudes of these sinks are comparable because the reaction rate of $O^+$ with $O_2$ is an order of magnitude larger than with $N_2$. The two sinks also have similar altitude and temporal behaviors because of their similar scale heights. Therefore, the peak electron density is proportional to the ratio of the atomic oxygen density to the effective molecular density ([O]/[M]).

According to Prolss (1980), it is now believed that positive storm effects are not related to density changes but are instead caused by ionization transport effects. In particular, a reduced poleward wind or an increased equatorward wind will increase the height of the layer ($H_mF_2$) and the [O]/[M] ratio and hence $N_mF_2$. At solar minimum, an increase of 50 km in $H_mF_2$ would lead to a factor of 2 increase in [O]/[M] at the peak and a similar increase in $N_mF_2$.

## MODEL

The model that has been employed in these calculations is a comprehensive model of the low energy thermal plasma in the ionosphere and plasmasphere of the Earth (Young et al., 1980a,b; Richards et al., 1983; Richards and Torr, 1985; Richards and Torr, 1986). The main component of this one-dimensional model calculates the plasma densities and temperatures along entire magnetic flux tubes from 80 km in the northern hemisphere through the plasmasphere to 80 km in the southern hemisphere. The model, which is called the Field Line Interhemispheric Plasma (FLIP) model, uses a tilted dipole approximation to the Earth's magnetic field. The equations solved are the continuity and momentum equations for $O^+$, $H^+$, and $He^+$, as formulated for the topside ionosphere by St. Maurice and Schunk (1976). Collisions between ions and neutrals have been included in order to extend the equations into the E and F regions.

The electron and ion temperatures are obtained by solving the energy equations (Schunk and Nagy, 1978). Electron heating due to photoelectrons is provided by a solution of the 2-stream photoelectron equations using the method of Nagy and Banks (1970). The solutions have been extended to encompass the entire field line on the same spatial grid as the ion continuity and momentum equations. With the latest cross sections and solar EUV fluxes as inputs, Richards and Torr (1984) have demonstrated that the model photoelectron fluxes are in good agreement with the measured fluxes of Lee et al. (1980).

The FLIP model calculates the vibrational distribution of $N_2$ in order to take into account the strong dependence of the $O^+ + N_2 \rightarrow NO^+ + O$ reaction rate on the degree of vibrational excitation of $N_2$. It has been shown previously by Richards and Torr (1986) that this effect may be important at solar maximum in

summer but is usually not important at other times under magnetically quiet conditions. Vibrationally excited $N_2$ is produced efficiently by photoelectron and thermal electron excitation and also by a number of chemical reactions but is quenched efficiently at low altitudes by atomic oxygen. We have investigated the possibility that the observed storm time decrease in $N_mF_2$ is due to vibrationally excited $N_2$ but the model indicates that the enhancement in the $O^+ + N_2$ reaction rate due to vibrational excitation of $N_2$ at the peak of the layer is 30% on both the prestorm day and the storm day and does not contribute to the reduction in $N_mF_2$ on this occasion. We normally employ a zero flux upper boundary condition to obtain the vibrational $N_2$ populations but we also simulated the possibility that the decrease in $N_mF_2$ resulted from vibrational $N_2$ produced in the auroral zone and transported to midlatitudes by inserting a downward flux at the upper boundary. Even with unrealistically large fluxes, the increase in the $O^+ + N_2$ reaction rate was small in the vicinity of the peak, although, large increases occured above the peak.

In order to simulate the ETS period, the FLIP model requires 3 key inputs: the solar EUV flux, the neutral atmosphere, and the meridional component of the neutral wind. These 3 inputs are discussed below.

The solar EUV flux is related to the level of solar activity which was very low during this solar minimum period as indicated by the 10.7 cm solar flux. The F10.7 index was 75 for the ETS period but the previous 2 months had been more active with an average F10.7 index of 86 for August and 92 for July. This level of solar activity is similar to the early months of 1974 for which solar EUV flux measurements are available. Therefore, we have adopted the F74113 solar EUV fluxes in the 37 wavelength intervals proposed by Torr et al. (1979) for the present calculations. The F10.7 index for day 113 of 1974 is 71 which

is very close to the value during the ETS period. We have made one modification to these fluxes based on the work of Richards and Torr (1984) who pointed out an inconsistency between the measured solar EUV flux and the measured photoelectron flux in the wavelength range below 250 Å. We have doubled the fluxes below 250 Å and this increases the ion production rates by about 10%.

To simulate magnetic storm effects on the neutral atmosphere, we use the MSIS86 model with the 3 hour Ap magnetic activity index option (Hedin, 1987). The Ap variation during this period is indicated by the full line in Figure 1; the dashed curve represents the Ap that was adopted in order to reproduce the observed decrease in $N_mF_2$. The time scale used in this figure is the time elapsed from midnight universal time on 16-17 September so the Ap in Figure 1 is for days 18, 19, and 20. This figure indicates that there was a large magnetic storm at 57 UT and 4.5 hours local solar time on 19 September when the Ap index rose to 80.

The meridional neutral wind affects the F2 layer peak density ($N_mF_2$) by affecting the rate by which the $O^+$ ions diffuse downward and this is reflected in the height of the layer. Normally the wind is poleward during the day, enhancing the downward diffusion to a region of increased loss, thereby reducing the peak density ($N_mF_2$) and lowering the height of the layer. At night the wind becomes equatorward, inhibiting the downward diffusion, raising the height of the layer and helping to maintain the nighttime F2 layer density. The measured height variation of the layer, from which the winds were deduced, is shown in Figure 2. $H_mF_2$ is not available between 32 and 38 hours and again between 74 and 82 hours. On the storm day, the daytime $H_mF_2$ exceeded that on the previous day by 40 km. The winds in these calculations were obtained from the height of the layer using the method of Miller et al. (1986). The winds for the ETS

period are presented in Buonsanto et al. (this issue). On the day before the storm, the wind was poleward during the sunlit period. The increased layer height on the storm day results from a reduction of the poleward wind on that day. During part of the daytime the wind has actually reversed to become equatorward. We note that the meridional wind derived from the layer height is likely to have an electric field component, especially on the storm day. However, this electric field can be treated as an effective neutral wind for our purposes. Also, winds deduced from $H_mF_2$ are sensitive to the neutral atmosphere which has a large uncertainty on the storm day. The observed decrease in $N_mF_2$ on the storm day suggests a larger change in the neutral densities than is indicated by the MSIS model. In our calculations with modified neutral densities, we modify the winds to reproduce the observed layer height.

## RESULTS

Figure 3 compares the measured variation of $N_mF_2$ at Millstone Hill with the $N_mF_2$ from the FLIP model, beginning at midnight local time on the day before the storm (18 September). There is generally very good agreement between the model and the data for the prestorm day with the model reproducing the observed evening enhancement in $N_mF_2$. The daytime model $N_mF_2$ is 20-30% lower than the measured density. The good agreement in the prenoon sector is actually an artifact because the height of the layer is not available and the neutral winds have been chosen to adjust the layer height to improve the overall agreement between the modeled and measured peak electron densities.

The good agreement on the prestorm day is not maintained on the storm day, however, when the model actually predicts a slight increase in $N_mF_2$ rather than the factor of 1.7 decrease. The increase in the model peak electron density on

the storm day is a response to the 40 km increase in layer height on the storm day. If there were no changes in the neutral atmosphere, a 40 km increase in layer height would produce a factor of two increase in $N_mF_2$. The actual increase is less than a factor of 2 as a result of the changes in neutral composition. Examination of the Ap variation in Figure 1 and the measured $N_mF_2$ in Figure 3 reveals a prompt response to the magnetic storm onset. The morphology of the ionospheric behavior in this storm is by no means unusual, being similar to that observed over Brisbane, Australia during the February 21-22, 1973 storm when the Ap increased to 50 just before sunrise (Prolss, 1980).

In order to investigate why the model does not reproduce the observed storm time behavior, we need to look at the changes in the neutral atmosphere resulting from the storm. We do not have direct measurements of the neutral densities but we do have the measured ion temperature which is expected to be close to the neutral temperature in the F region because there is close coupling between the ions and neutrals. The F region measured ion temperature during this period is compared with the MSIS neutral temperature in Figure 4. For most of the period, there is reasonable agreement between the measured ion temperature and MSIS model neutral temperature but the measured ion temperature is very low in the post midnight sector where it is 150°K lower than the MSIS neutral temperature before the onset of the storm. The ion temperature and MSIS neutral temperature would be expected to be in better agreement during this quiet period and the reason for this discrepancy is not known. On the morning after the storm, the ion temperature is about 150°K greater than the neutral temperature.

In order to bring the ion and neutral temperatures into closer agreement on the storm day we have increased the severity of the storm by increasing the Ap in the first 6 hours from 80 to 200 as indicated by the broken line in Figure 1. Such an approach can be justified on the basis of the known variability of magnetic storms which cannot be adequately incorporated in empirical neutral atmosphere models such as MSIS-86. The resulting change in the neutral densities is shown in Figure 5 for 300 km altitude. This change did result in a decrease in $N_mF_2$ but in order to obtain the full observed decrease we also had to normalize the O density so that there was no increase over the previous day at 300 km. The O scale height was still consistent with the neutral temperature on the storm day however, and consequently, the densities above and below 300 km are different.

This type of behavior of O is not unusual during storms. Measurements presented by Prolss (1980) for other storms indicate that during some storms the O density at 300 km often remains steady or even decreases during the negative phase of a magnetic storm. A factor of 3-4 decrease in the ratio of O to $N_2$ at 300 km was necessary to produce the observed decrease in $N_mF_2$ of a factor of 1.7. The increase in the $O_2$ densities was a factor of 4-5. The resultant $N_mF_2$ variation is shown in Figure 6. One interesting point in this figure is that the measurements appear to show that the ionosphere has almost fully recovered on the day after the storm whereas the model is still showing a reduced density. The MSIS neutral densities in Figure 6 are still much higher on the day after the storm than on the quiet day even when the smaller Ap is used.

Figure 7 shows a comparison between the measured electron temperature and the model electron temperature corresponding to the electron densities in Figure 6. The agreement is good for the time on the quiet day when data is available.

Unfortunately, there is a gap in the data near sunrise where the model indicates a peak in the electron temperature. In the F region, the main sink for electron energy is coulomb collisions with the ions. As a result, the electron temperature is dependent on the square of the electron density. The very low pre-sunrise electron densities are responsible for the rapid increase in electron temperature. The sensitivity of the electron temperature to the electron density is clear when comparing the model temperatures on the quiet and storm day. The factor of 2 decrease in $N_mF_2$ results in a $500^oK$ rise in electron temperature. The measured electron temperature shows a much smaller rise in electron temperature on the storm day than the model even though the measured decrease in electron density is greater than the model decrease.

## CONCLUSIONS

The FLIP model reproduces the quiet time behavior of the electron density and temperature at Millstone Hill very well during the September equinox at solar minimum. The storm time behavior is not well modeled, possibly as a result of the inability of the MSIS-86 model to produce the correct neutral densities for this particular storm. A factor of 3-5 increase in the ratio of the atomic oxygen density to molecular densities at 300 km is needed to explain the observed decrease in $N_mF_2$; double the increase in the ratio indicated by the MSIS-86 model using the true Ap history. We also investigated the possibility that vibrationally excited $N_2$ could enhance the storm effects but it was found to be unimportant.

Acknowledgments. This work was supported by NSF grants ATM-8713693, ATM-8716036, and ATM-8714461; and NASA grants NAGW-922, and NAGW-996 at The University of Alabama in Huntsville. Millstone Hill data were acquired and analysed under the support of NSF cooperative agreement ATM-8808137 to Massachusetts Institute of Technology. Support for K.L. Miller was provided by NSF grant ATM-8715367.

## REFERENCES

Hedin, A.E., MSIS-86 thermosphere model, J. Geophys. Res., 92, 4649, 1987.

Lee, J. S., J. P. Doering, T. A. Potemra and L. H. Brace, Measurements of the ambient photoelectron spectrum from Atmosphere Explorer: I. AE-E measurements below 300 km during solar minimum conditions, Planet. Space Sci., 28, 947, 1980.

Miller, K.L., D.G. Torr, and P.G. Richards, Meridional winds in the thermosphere derived from measurement of F2-layer height, J. Geophys. Res., 91, 4531, 1986.

Nagy, A. F. and P. M. Banks, Photoelectron fluxes in the ionosphere, J. Geophys. Res., 75, 6260, 1970.

Prolss, G. W., Magnetic storm associated perturbations of the upper atmosphere: recent results obtained by satellite-borne gas analyzers, Rev. Geophys. Space Phys., 18, 183, 1980.

Richards, P. G., and D. G. Torr, An investigation of the consistency of the ionospheric measurements of the photoelectron flux and solar EUV flux, J. Geophys. Res., 89, 5625, 1984.

Richards, P. G., R. W. Schunk, and J. J. Sojka, Large-scale counterstreaming of $H^+$ and $He^+$ along plasmaspheric flux tubes, J. Geophys. Res., 88, 7879,

1983.

Richards, P. G. and D. G. Torr, Seasonal, diurnal, and solar cyclical variations of the limiting $H^+$ flux in the Earth's topside ionosphere, J. Geophys. Res., 90, 5261, 1985.

Richards, P. G., and D.G. Torr, A factor of 2 reduction in the theoretical F2 peak electron density due to enhanced vibrational excitation of $N_2$ in summer at solar maximum, J. Geophys. Res., 91, 11331, 1986.

Schunk, R. W., and A. F. Nagy, Electron temperatures in the F region of the ionosphere: Theory and observations, Rev. Geophys. Space Phys., 16, 355, 1978.

Seaton, M. J., A possible explanation of the drop in F-region critical densities accompanying major ionospheric storms, J. Atmos. Terr. Phys., 8 122, 1956.

St. Maurice, J.-P., and R. W. Schunk, Diffusion and heat flow equations for the mid-latitude topside ionosphere, Planet. Space Sci., 25, 907, 1976.

Torr, M. R., D. G. Torr, R. A. Ong, and H. E. Hinteregger Ionization frequencies for major thermospheric constituents as a function of solar cycle 21, Geophys. Res. Lett., 6, 771, 1979.

Young, E. R., P. G. Richards and D. G. Torr, A flux preserving method of coupling first and second order equations to simulate the flow of plasma between the protonosphere and the ionosphere, J. Comp. Phys., 38, 141, 1980a.

Young, E. R., D. G. Torr, P. Richards, and A. F. Nagy, A computer simulation of the midlatitude plasmasphere and ionosphere, Planet. Space Sci., 28, 881, 1980b.

## FIGURE CAPTIONS

Fig.1. The 3 hour Ap variation during the period 18-20 September 1984 (full line) showing the period of low Ap on 18 September followed by a large increase on 19 September and a return to moderate activity on 20 September. The broken line represents the Ap used to explain the observed decrease in $N_mF_2$.

Fig.2. The measured height of the F2 region peak electron density ($H_mF_2$). The dashed lines indicate periods where there are gaps in the data. The dashed curves were obtained from the model in fitting the observed $N_mF_2$. Note the approximately 40 km larger $H_mF_2$ on 19 September at local noon (60 hours approx.) and local noon on 18 September (40 hours).

Fig.3. Comparison of the model $N_mF_2$ (broken line) with the measured $N_mF_2$ (full line). The model reproduces the quiet day variation well with a prominent evening enhancement. On the storm day, the model gives a slight increase rather than the decrease in $N_mF_2$ indicated by the measurements.

Fig.4. Comparison of the measured ion temperature (full line) with the MSIS-86 exospheric neutral temperature (broken line). The ion temperature is 150°K lower than the MSIS-86 neutral temperature just before the storm, whereas, the neutral temperature is 200°K lower than the ion temperature just after the storm onset.

Fig.5. The neutral density variation at 300 km for the 2 different Ap histories shown in Figure 1. The larger densities result from the modified Ap. The modified Ap generates molecular densities that are a factor of 3-5 larger on the storm day than on the quiet day for several hours after the storm commencement. Although the densities remain high on 20 September compared to the quiet day, the difference between the densities for the two sets of Ap is small.

Fig.6. Comparison of the measured (full line) and modeled $N_mF_2$ (broken line) with the modified Ap history, and the O density restrained to follow the diurnal variation on 18 September.

Fig.7. Comparison of the model electron temperature (broken line) variation with the measured temperature variation (full line) for the model electron densities

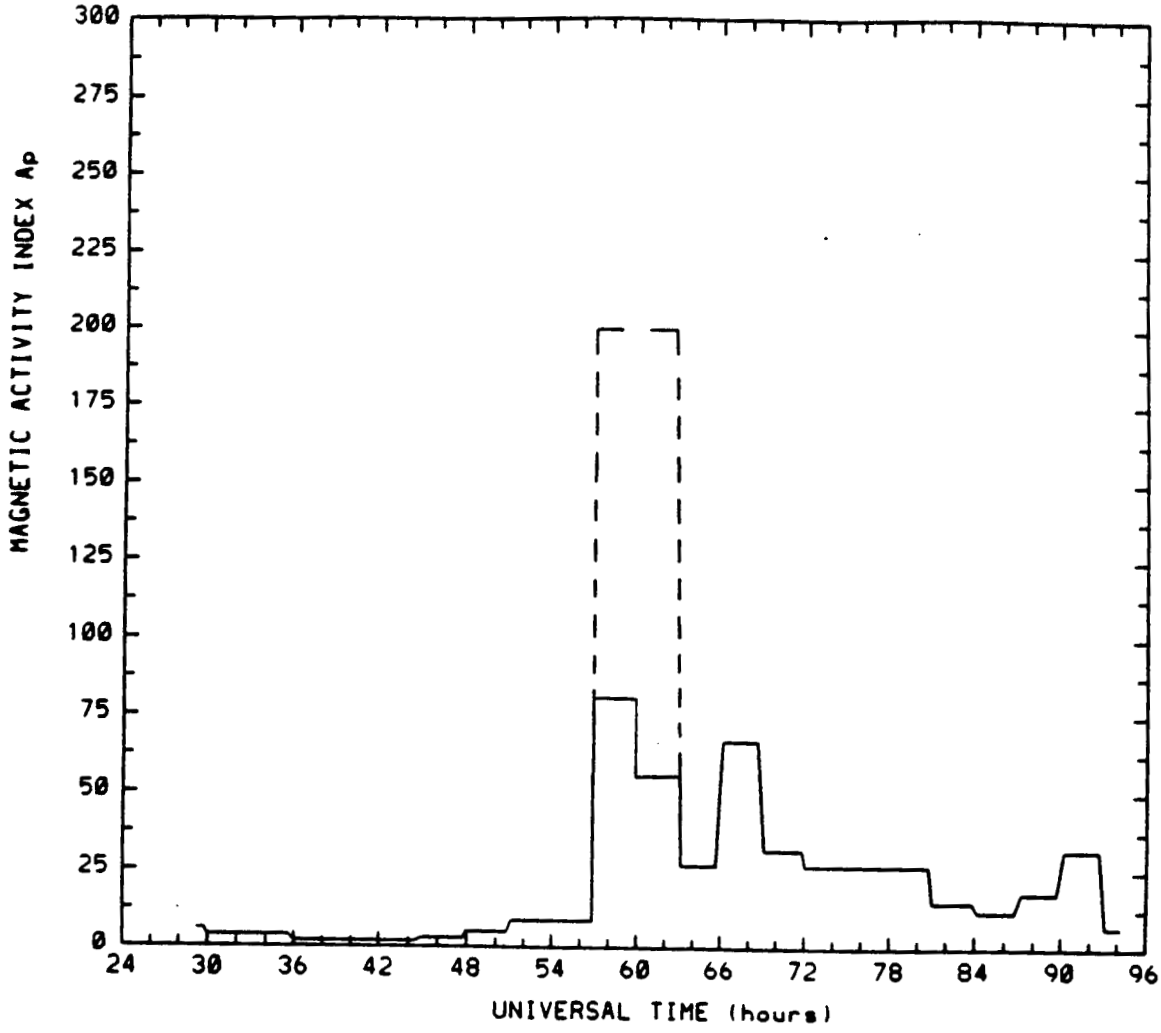


Fig.1. The 3 hour Ap variation during the period 18-20 September 1984 (full line) showing the period of low Ap on 18 September followed by a large increase on 19 September and a return to moderate activity on 20 September. The broken line represents the Ap used to explain the observed decrease in $N_mF_2$.

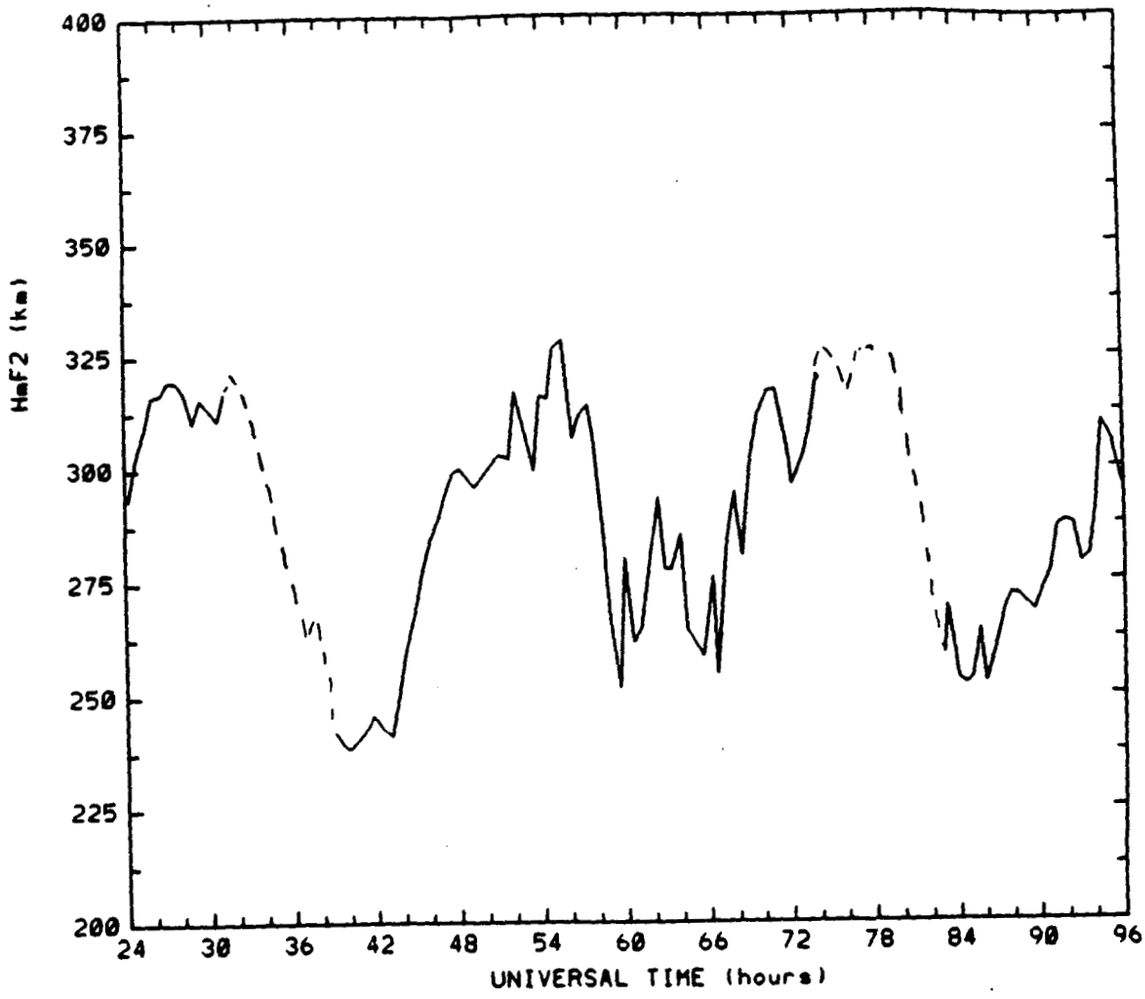


Fig.2. The measured height of the F2 region peak electron density ($H_mF_2$). The dashed lines indicate periods where there are gaps in the data. The dashed curves were obtained from the model in fitting the observed $N_mF_2$. Note the approximately 40 km larger $H_mF_2$ on 19 September at local noon (60 hours approx.) and local noon on 18 September (40 hours).

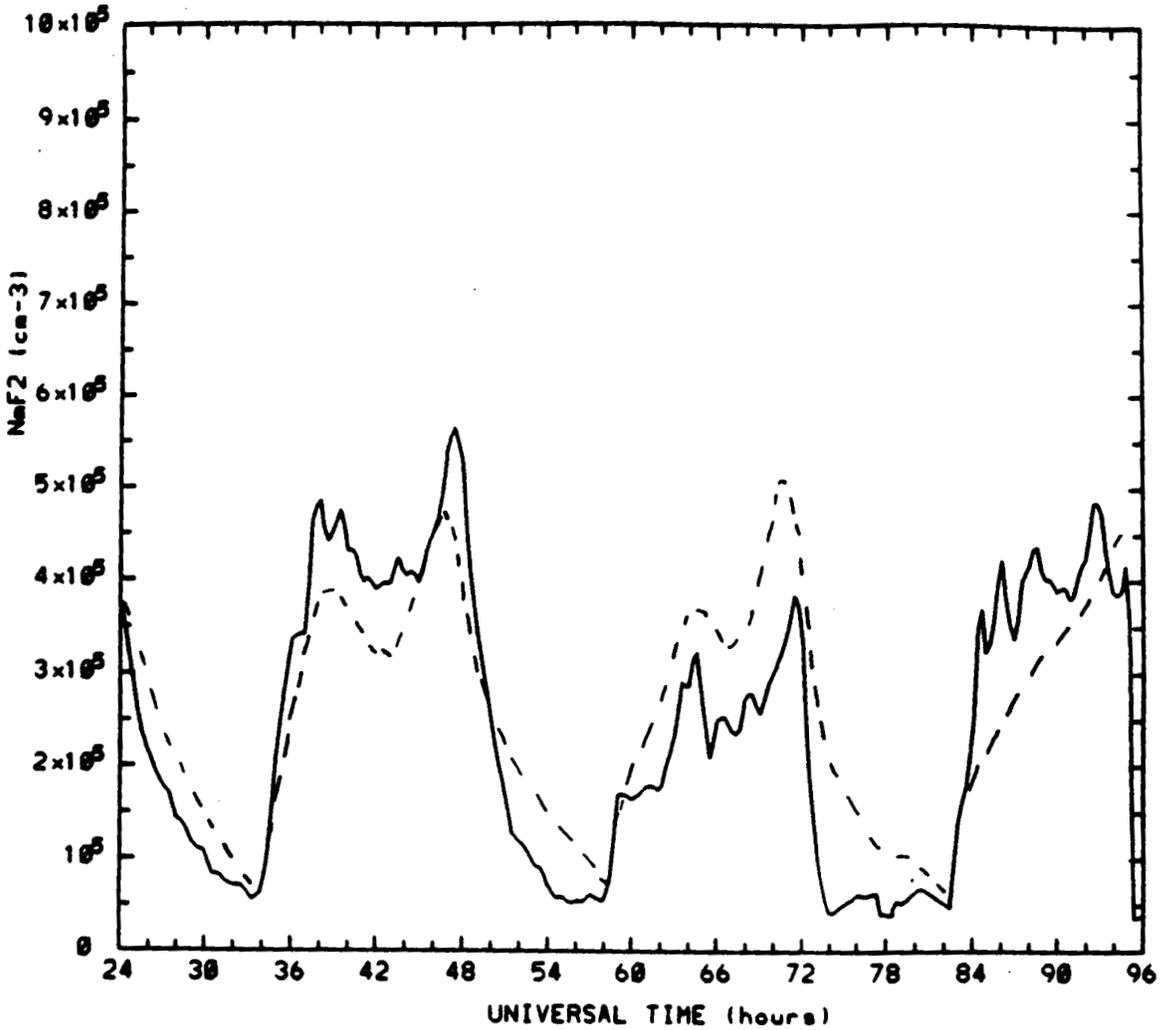


Fig.3. Comparison of the model $N_mF_2$ (broken line) with the measured $N_mF_2$ (full line). The model reproduces the quiet day variation well with a prominent evening enhancement. On the storm day, the model gives a slight increase rather than the decrease in $N_mF_2$ indicated by the measurements.

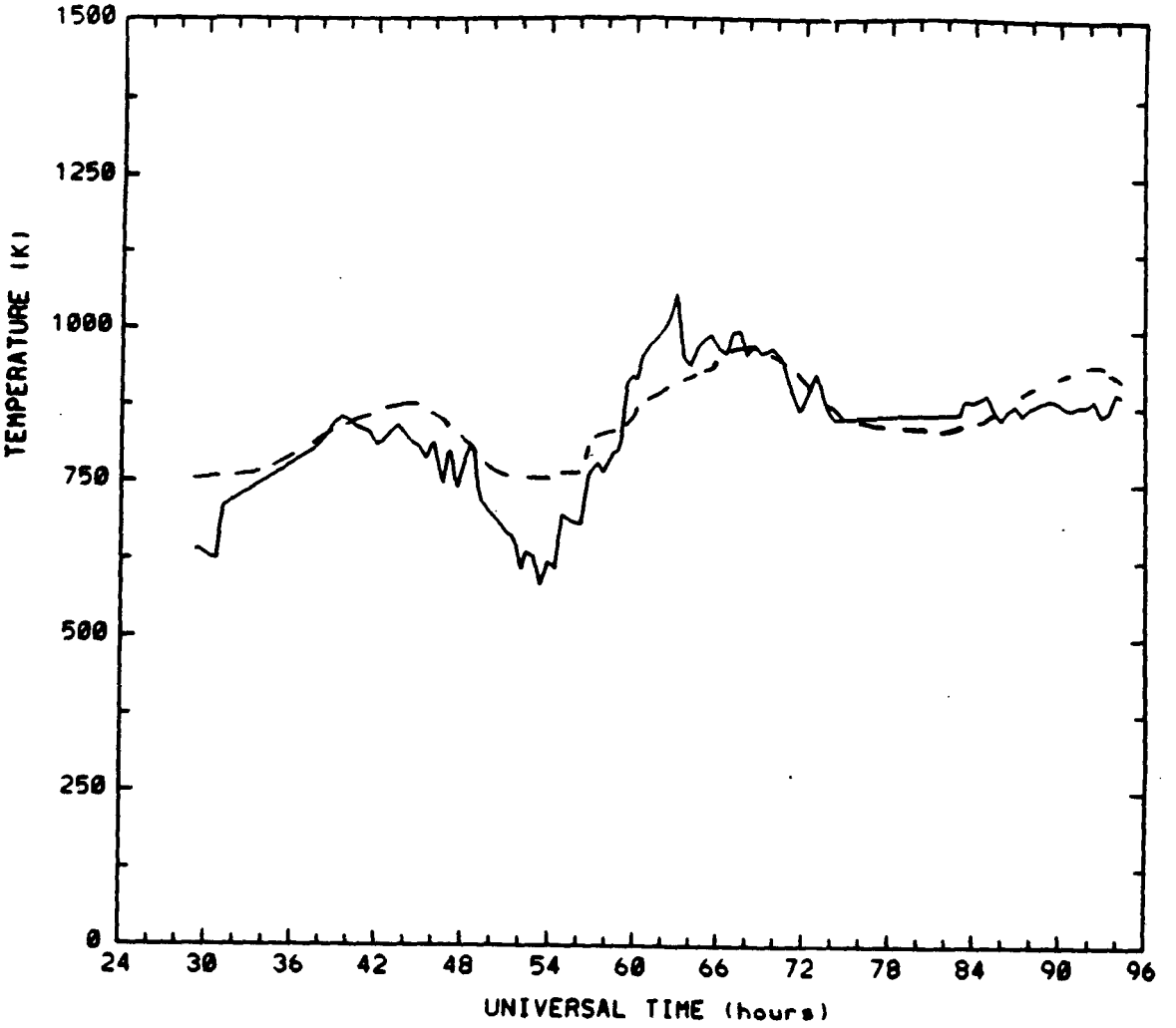


Fig.4. Comparison of the measured ion temperature (full line) with the MSIS-86 exospheric neutral temperature (broken line). The ion temperature is 150°K lower than the MSIS-86 neutral temperature just before the storm, whereas, the neutral temperature is 200°K lower than the ion temperature just after the storm onset.

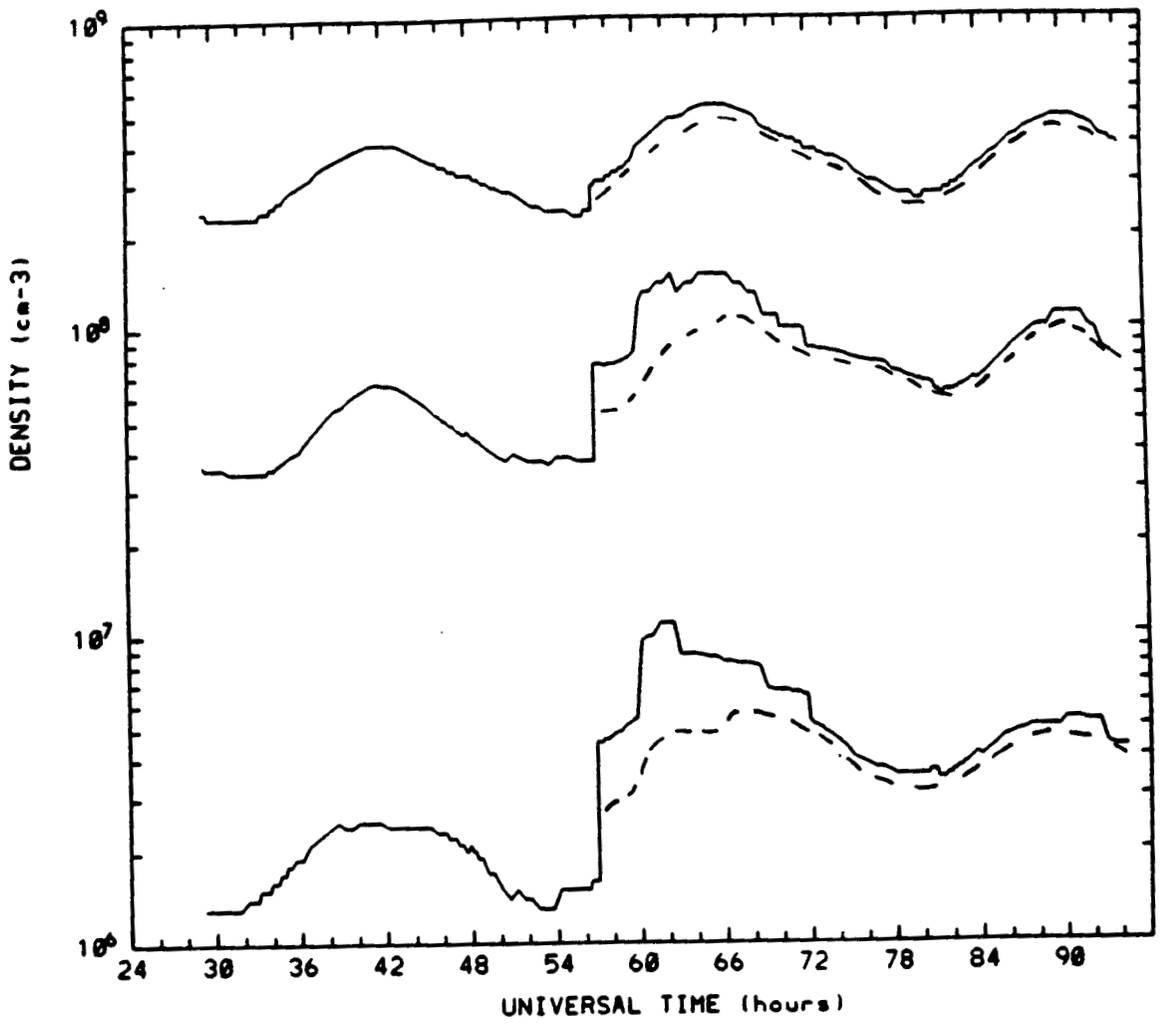


Fig.5. The neutral density variation at 300 km for the 2 different Ap histories shown in Figure 1. The larger densities result from the modified Ap. The modified Ap generates molecular densities that are a factor of 3-5 larger on the storm day than on the quiet day for several hours after the storm commencement. Although the densities remain high on 20 September compared to the quiet day, the difference between the densities for the two sets of Ap is small.

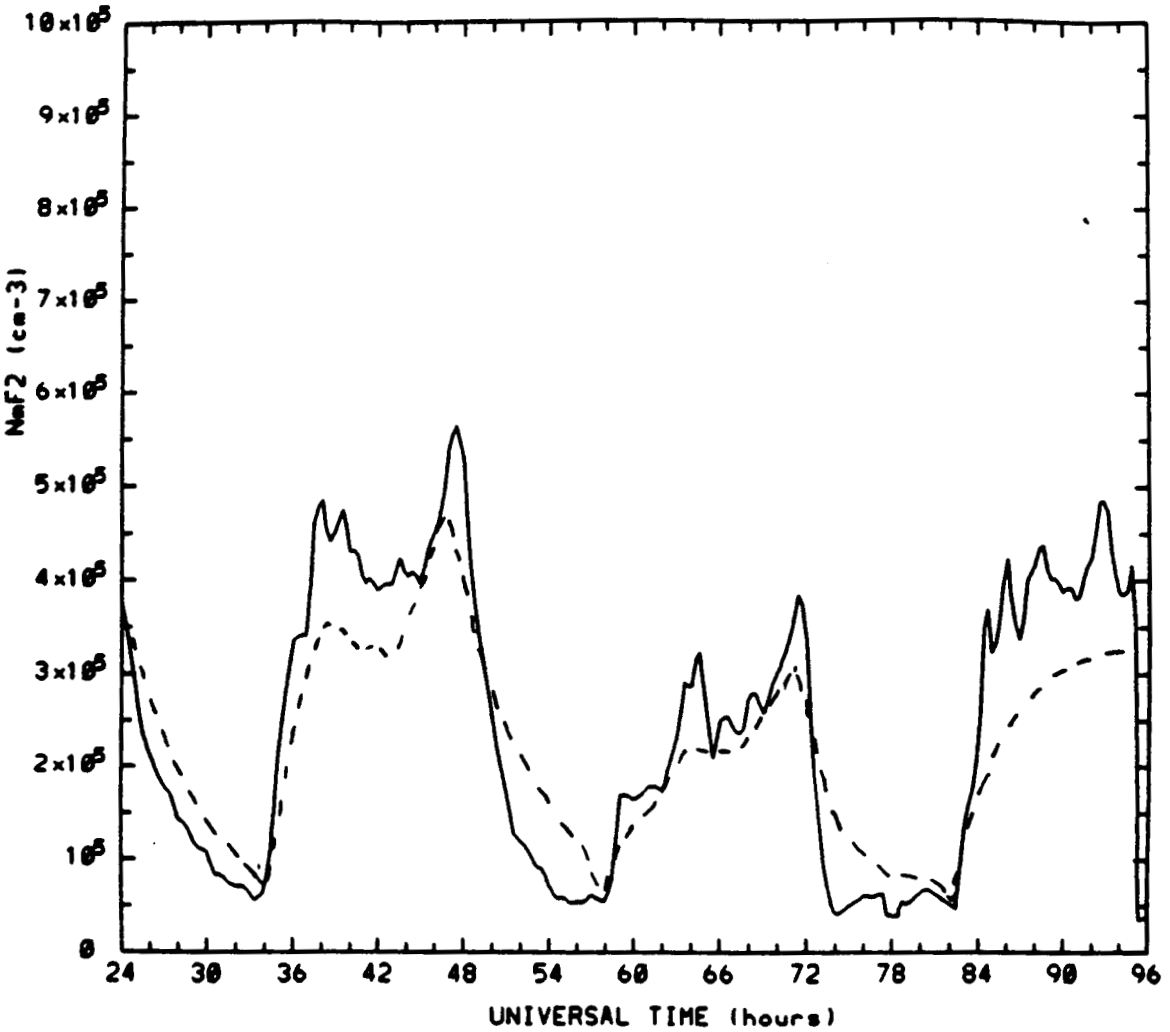


Fig.6. Comparison of the measured (full line) and modeled $N_mF_2$ (broken line) with the modified Ap history, and the O density restrained to follow the diurnal variation on 18 September.

Fig 6

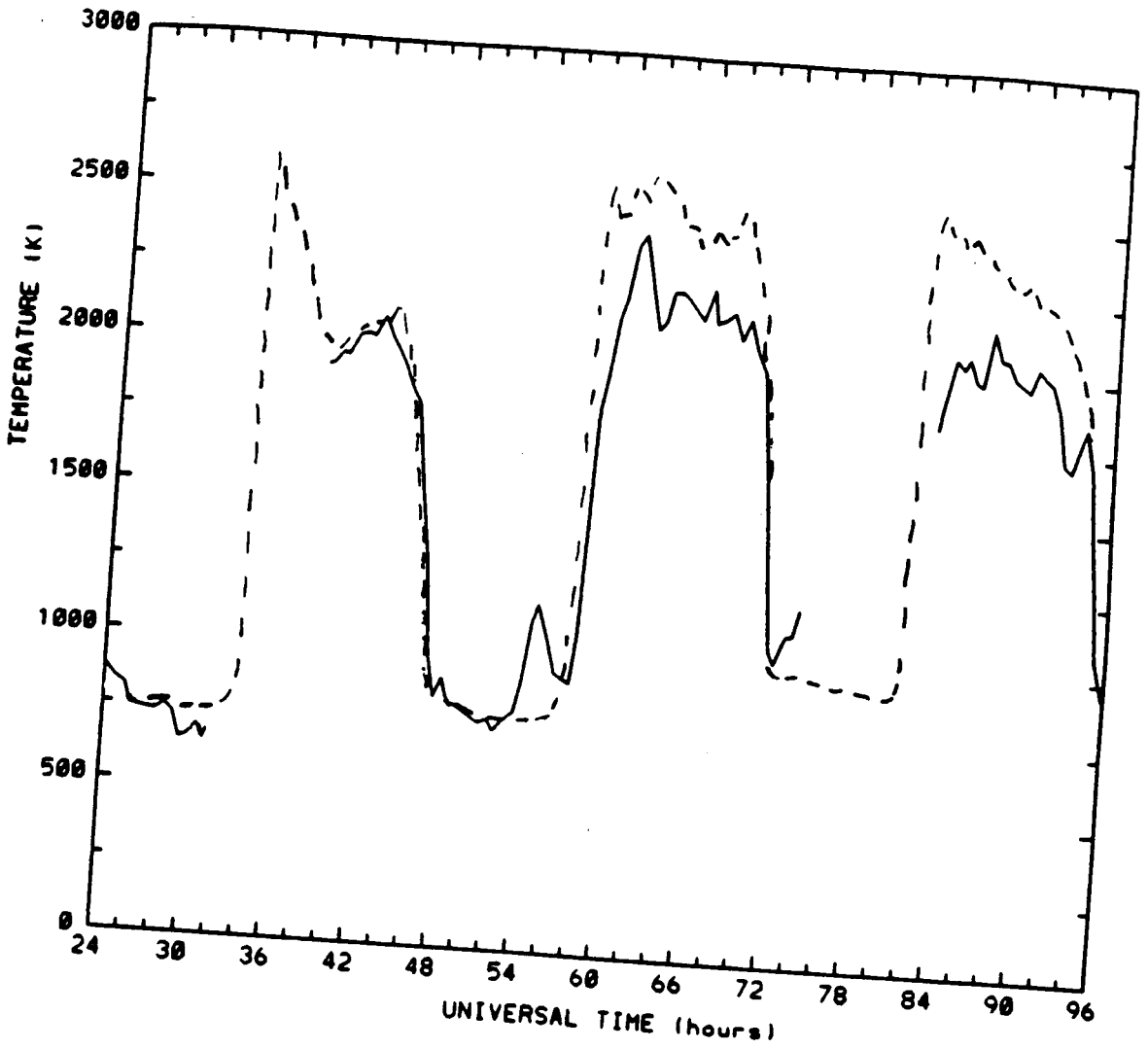


Fig.7. Comparison of the model electron temperature (broken line) variation with the measured temperature variation (full line) for the model electron densities